難な分子であったため、CL 蛋白質と CL binder の直接的相互作用を解析するためには pull down 法等の煩雑な手法を選択せざるを得なかった。今回

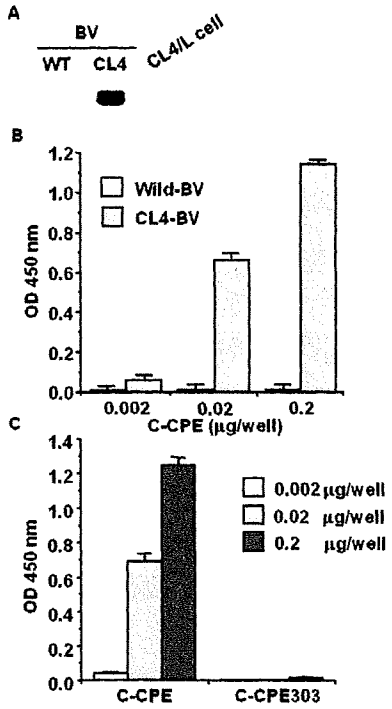

Figure 1 Preparation of CL4-displaying BV
A) Western blot analysis. Mock-BV and CL4-BV (0.1 μg/lane) were subjected to SDS-PAGE, followed by immunoblot analysis with anti-CL4 Ab. The lysate of CL4-expressing L (CL4/L) cells was used as a positive control. B, C) Interaction of a CL4 binder with CL4-BV. Immunotubes were coated with the mock-BV or CL4-BV, and C-CPE (B) or mutated C-CPE (C) was added to the BV-coated immunotubes at the indicated concentration. C-CPE bound to the BV-coated tubes was detected by ELISA with an anti-his tag Ab. Data are means ± SD (n=4).

作製した CL-BV は CL binder スクリーニング系への応用のみならず、CL binder と CL 蛋白質との直接的相互作用を ELISA 法いう簡便な解析方法に応用できる点においても有用であると考えられる。

C-2. CL binder スクリーニング系の構築

ファージディスプレイ法はターゲット分子に対する結合分子を網羅的かつ迅速に同定できる技術として開発され、抗体や機能性人工蛋白質の創出に現在広く応用されており、ファージディスプレイ法を用いたスクリーニングにより、CL binderを創出しうる可能性が示唆される。実際、近年になってLingらが12 mer peptideライブラリとCL4発現細胞を用いてCL4 結合ペプチドを取得した例も報告されている。そこで、ファージディスプレイライブラリをCL binderスクリーニング系へ応用することを考慮して、CL4 binderであるC-CPEをファージ表面に提示させたC-CPEファージとCL4-BVの相互作用をELISA法により解析した。

C-CPEファージは濃度依存的にCL4-BVに結合性を示し、WT-BVには結合性を示さなかった。またCL4の非結合性分子である一本鎖抗体scFvを提示させたscFvファージはCL4-BV, WT-BVの双方に結合性を示さなかった（Fig. 2A）。以上のことからC-CPEファージはCL4-BVへの特異的な結合性を保持しており、CL-BVを利用することでCL 結合性ファージのスクリーニングが行えるものと推察される。

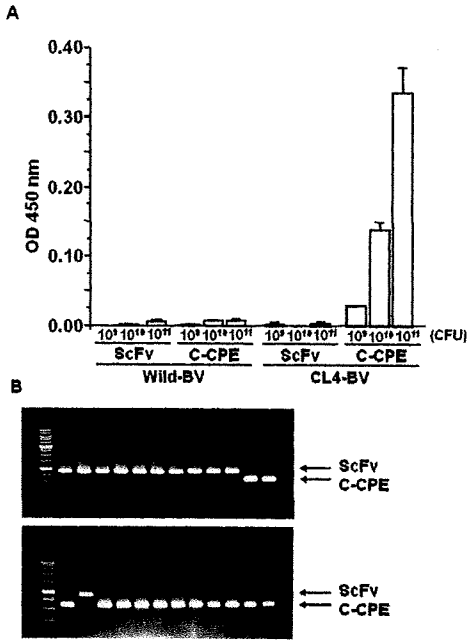

Figure 2 Selection of C-CPE-displaying phage by using the CL4-BV system. A) Interaction of C-CPE-displaying phage with CL4-BV. Mock-BV or CL4-BV was coated on an immunoplate, and then scFv-displaying phage or C-CPE-displaying phage was added to the BV-coated immunoplate at the indicated concentrations. The BV-bound phages were detected by ELISA with anti-M13 Ab. Data are means ± SD (n=3). B) Enrichment of C-CPE-displaying phage by the BV system. A mixture of scFv-phage and C-CPE-phage (mixing ratio of scFv-phage to C-CPE-phage = 2:10) was incubated with a CL4-BV-coated immunotube, and the bound phages were recovered. Each phage clone was identified by PCR amplification, followed by agarose gel electrophoresis. Upper and lower pictures are before and after the selection, respectively. The putative sizes of the PCR products are 856 and 523 bp in scFv and C-CPE, respectively.

そこで次に、C-CPE 及びCL4 をそれぞれCL binder、CL のモデルとして用い、CL-BV を利用したCL binderスクリーニング系が機能するかを検討した。CL4 非結合分子であるscFv ファージとCL4 binderであるC-CPEファージを10:2の割合で混合したファージ溶液を調整した（Input）。mCL4-BVを固相化したイムノチューブに調整したファージ溶液を添加し、洗浄、溶出操作を行った後に結合したファージクローンを回収し（Output）、選別操作前後のscFvファージおよびC-CPEファージの存在比をCD-PCR法により解析した。

選別操作前には 12 クローン中 2 クローンであった C-CPE ファージは選別操作後 12 クローン中 11 クローンに増加しており（Fig. 2B）、BV を用いた CL binder スクリーニング系が機能することが示唆された。

C-3. CL-1 結合性ファージのスクリーニング

当研究グループでは C-CPE の C 末端 16 アミノ酸のアラニンスキャンにより、CL-4 結合に関与するアミノ酸を複数同定している。そこで、本機能アミノ酸をランダムに変異させた C-CPE 誘導体ライブラリを作製した（尚、特許の関係で配列情報は示さず）。pET-H10PER に導入された C-CPE を鋳型として NNS 配列を導入したプライマーを用いて PCR 反応を行い、PCR 産物を pY03' ファージミドベクター（医薬基盤研究所堤康央博士より供与）にライゲーションした後、本 plasmid を用いて大腸菌 TG-1 に形質転換しライブラリを作成した。さらにライブラリの多様性を確認するために任意のクローンを選択しシークエンス解析を行った。

シークエンス解析の結果、いずれのクローンも野生型と異なる配列を有しており、ライブラリが多様性を有していることが示された（data not shown）。またライブラリサイズは 1.4×10^7 CFU であり、理論値である 6.4×10^7 CFU に近い多様性を有するライブラリを作製することができた。そこで、次に、本ライブラリを用いた CL1 binder スクリーニングを試みた。

パンニングのラウンドを重ねるごとに濃縮率（ratio）の向上が観察され、CL1-BV に親和性を有するクローンが濃縮されたことが示唆された（Fig. 3A and 3B）。以前に CL 非発現細胞であるマウス繊維芽細胞に CL を導入した発現細胞を用いて C-CPE 誘導体ライブラリをパンニングしたが、このような段階的な ratio の向上は観察されなかったため（data not shown）、本結果は CL-BV を用いることで CL binder が効率的にスクリーニングできたものと推察される。

パンニングにより濃縮率の向上が認められ、CL1 に親和性を持つファージが濃縮された。そこで CL1 親和性分子を同定するためにパンニング後のファージ群を個々にモノクローン化し、ELISA 法によって各クローンの CL1 結合性を解析した。3rd round 後のファージクローンを解析した結果、数多くの CL1 親和性クローンが観察された（Fig. 3C）。

さらに、シークエンス解析により、配列の異なる 2 つの CL1 結合性ファージクローン（A、B）の取得に成功した（特許の関係上、配列データは示さず）。

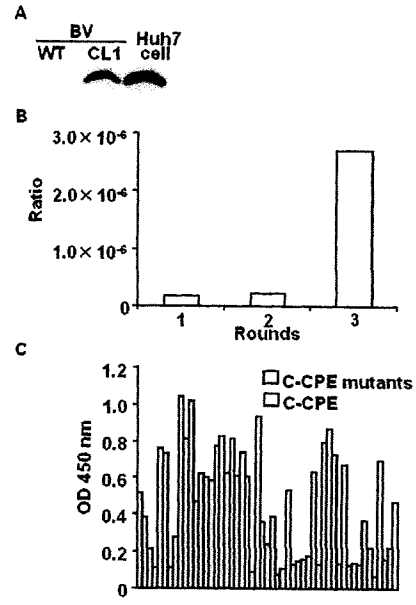

Figure 3 Screening of a CL1 binder.
A) Preparation of CL1-BV. Wild-BV and CL1-BV (0.1 μg/lane) were subjected to SDS-PAGE, followed by immunoblot analysis with anti-CL1 Ab. The lysate of Huh7 cells was used as a positive control. B) Enrichment of phages with affinity to CL1-BV. CL1-BV coated on immunotubes were incubated with the C-CPE-derivative phage library at 3.2×10^{12} CFU titer (1st input phage). The phages bound to CL1-BV were recovered (1st output phage). The CL1-BV-binding phages were subjected to two additional cycles of the incubation and wash step, resulting in 2nd, 3rd output phage. The ratio of output phage to input phage titers was calculated. C) Monoclonal analysis of C-CPE mutant phage. CL1-BV-bound phage clones were isolated from the 3rd output phages, and the interaction of the monoclonal phage with CL1-BV was examined by ELISA with HRP-anti-M13 Ab as described in Materials and methods. The most right column indicates C-CPE-phage.

C-4. CL1 binder の作製

目的の C-CPE mutant A/B 遺伝子がコードされているファージミドベクター、pY03-C-CPEmutant を鋳型とし、制限酵素サイトとして *Nde*I/*Bam*HI を持つ primer を用いて、PCR により C-CPE mutant 配列を増幅した。制限酵素処理後、His-tag 融合蛋白質発現ベクターである pET-16b に組み込み、*Xho*I 処理によって目的組換え産物以外を消化した。シークエンス確認を行い目的の組換え plasmid の作製を確認した。次に、A および B の蛋白質発現誘導条件、可溶化条件、蛋白質溶出条件を設

定し、蛋白質の精製を行ったところ、推定される分子量に CBB 染色像が観察された(Fig. 4A)。

次に、CL1-BV を用いた ELISA により CL1 結合性を解析したところ、C-CPE では CL1-BV にほとんど結合性が観察されなかったのに対して、C-CPE mutant A/B は共に CL1-BV にのみ結合性が観察された(Fig. 4B)。

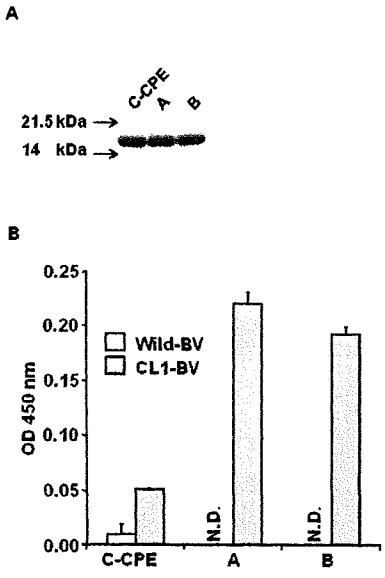

Figure 4 Interaction of C-CPE mutants with CL1-BV.
A) Purification of A and B. C-CPE mutants were expressed in *E. coli* and isolated by nickel-affinity chromatography. The purification of proteins was confirmed by SDS-PAGE. The putative molecular mass of C-CPEs is approximately 15 kDa. B) Interaction of the C-CPE mutants with CL1. C-CPE mutants (2.0 μg) were added to Wild-BV- or CL1-BV-coated immunoplates, followed by detection of C-CPE mutants bound to each BVs. Data are means ± SD (n=3).

D. 考察

本分担研究では、膜蛋白質を機能及び立体構造を保持した状態でウイルス表面に提示することが近年報告された BV 膜蛋白質発現系を利用して CL binder スクリーニング系構築を試みた。CL4 binder である C-CPE と CL4-BV の相互作用を ELISA 法により解析したところ、C-CPE は WT-BV、CL1-BV には結合せず、濃度依存的に、特異的に CL4-BV に結合したことから、BV 上で CL は少なくとも C-CPE と結合性を有する立体構造を保持した状態で発現していることが示唆された。そこで次に、CL4 binder(C-CPE)を提示した C-CPE ファージと CL4-BV との相互作用を解析したところ、negative control ファージでは CL4-BV に結合せず、C-CPE ファージは添加濃度依存的な結合性を示していた。このとき、C-CPE ファージは WT-BV に結合していなかった。以上結果から、CL-BV が CL binder スクリーニング系として応用可能である可能性が示唆された。

そこで研究終盤において、C-CPE の機能ドメインをランダムなアミノ酸に置換した C-CPE 変異体ライブラリを用いて CL1 binder のスクリーニングを行い、CL1 に結合性を示す C-CPE 変異体の取得に初めて成功した。

E. 結論

本研究は、独自のCL binder研究を有効活用し、近年新たにHCV受容体として同定されたCL-1を標的とした初めてのHCV感染阻害薬を創出することを目的としている。

平成20年度の成果を踏まえ、平成21年度は、①CL1 binderスクリーニング系の構築を行い、②本スクリーニング系を用いてCL1 binderの取得を試み、以下の成果を得た。

①CL1 binderのスクリーニング系の構築

C-CPE構造変異体ライブラリの中からCL1 binderをスクリーニングするために、CL1、2、3、4、5発現細胞、CLをウイルス膜上に提示した出芽バキュロウイルス(BV)を作製した。C-CPEはCL4発現細胞およびCL4-BVに特異的に結合すること、CL4-BVによりC-CPE提示ファージが特異的に濃縮することを見出し、CL-BVを利用したCL binderスクリーニング系を構築した。尚、CL発現細胞を用いたスクリーニングでは非特異的な結合が多くCL binder探索系としての利用は困難であった。

②CL1 binderの取得

CL1-BVをパンニングソースとして用いてCL1 binderのスクリーニングを試みたところ、CL1結合性を示すC-CPE誘導体提示ファージが単離された。本ファージのシークエンスデータを基にC-CPE誘導体蛋白質を作製し、CL1結合性を解析したと

ころ、本C-CPE変異体はCL1結合性を有していた。

上記の成果を踏まえ平成 22 年度は、引き続き CL-1 binder の作製を進めると同時に、CL-1 binder の HCV 感染阻害活性を解析する予定である。

F. 健康危険情報

該当事項なし

G. 研究発表

G-1 論文発表

1. Matsuhisa K, Kondoh M, Takahashi A and Yagi K (2009) Tight junction modulator and drug delivery. *Expert Opin Drug Deliv* **6**(5):509-515.

2. Saeki R, Kondoh M, Kakutani H, Tsunoda S, Mochizuki Y, Hamakubo T, Tsutsumi Y, Horiguchi Y and Yagi K (2009) A novel tumor-targeted therapy using a claudin-4-targeting molecule. *Mol Pharmacol* **76**(4):918-926.

3. 近藤昌夫、高橋梓、佐伯理恵、八木清仁、生体バリアを利用した創薬研究、Drug Delivery System, 24, 532-537, 2009.

4. Kakutani H, Kondoh M, Saeki R, Fujii M, Watanabe Y, Mizuguchi H and Yagi K (in press) Claudin-4-targeting of diphtheria toxin fragment A using a C-terminal fragment of *Clostridium perfringens* enterotoxin. *Eur J Pharm Biopharm.*

5. Kakutani H, Kondoh M, Fukasaka M, Suzuki H, Hamakubo T and Yagi K (in press) Mucosal vaccination using claudin-4-targeting. *Biomaterials.*

G-2 学会発表

1. 生体バリアを利用した薬物送達研究
近藤昌夫(阪大院薬)
日本薬剤学会第 25 年会、平成 21 年 5 月 21-23 日、静岡

2. 生体バリアの分子基盤を利用した創薬研究
近藤昌夫(阪大院薬)
第 25 回日本 DDS 学会学術集会、平成 21 年 7 月 3、4 日、東京

3. 生体バリアの分子基盤を利用した経粘膜 DDS
近藤昌夫、八木清仁(阪大院薬)
第 25 回日本 DDS 学会学術集会、平成 21 年 7 月 3、4 日、東京

4. Claudin を利用した創薬研究の可能性
近藤昌夫(阪大院薬)
彩都バイオサイエンスセミナー 、平成 21 年 10 月 15 日、大阪

5. 創薬ターゲットとしてのタイトジャンクションの可能性
近藤昌夫、八木清仁(阪大院薬)
創剤フォーラム 第 15 回シンポジウム「タイトジャンクションをめぐる最近の研究成果と創薬への応用」、平成 21 年 10 月 23 日、東京

6. A novel type of absorption enhancer, claudin-4 modulator
Koji Matsuhisa, Ryota Okude, Masuo Kondoh and Kiyohito Yagi
36rd annual meeting & exposition of the Controlled Release Society, July 18-22, 2009, Copenhagen, Denmark.

7. Claudin as a target molecule for mucosal absorption of peptide drug
Masuo Kondoh, Hiroshi Uchida, Takeshi Hanada, Kiyohito Yagi, 49th annual meeting of the

American society of cell biology, Dec 5-9, 2009, San Diego, USA.

8. Development of a novel screening system for claudin binder using baculovirus display.
Toshiaki Yamaura, Azusa Takahashi, Hideki Kakutani, Masuo Kondoh, Toshiko Sakihama, Takao Hamakubo, Kiyohito Yagi, 49th annual meeting of the American society of cell biology, Dec 5-9, 2009, San Diego, USA

9. Preparation of a controllable RNA polymerase I-dependent expression vector
Takeshi Yoshida, Manabu Ojima, Masuo Kondoh, Hiroyuki Mizuguchi, Kiyohito Yagi, 49th annual meeting of the American society of cell biology, Dec 5-9, 2009, San Diego, USA

10. Claudin-4を介した新規粘膜ワクチンの創製
鈴木 英彦、角谷 秀樹、深坂 昌弘、近藤 昌夫、八木 清仁(阪大院薬)、日本薬学会第130年会、平成22年3月、岡山

11. 出芽バキュロウィルスを用いた claudin binder スクリーニング系の構築
松下 恭平[1]、角谷 秀樹[1]、高橋 梓[1]、山浦 利章[1]、浜窪 隆雄[2]、近藤 昌夫[1]、八木 清仁[1]([1]阪大院薬、[2]東大先端研)、日本薬学会第130年会、平成22年3月、岡山

12. ウエルシュ菌エンテロトキシン断片をプロトタイプとした新規claudin-4 modulatorの創製
各務 洋平[1]、山浦 利章[1]、松下 恭平[1]、高橋 梓[1]、内田 博司[2]、花田 雄志[2]、松久 幸司[1]、渡利 彰浩[1]、近藤 昌夫[1]、八木 清仁[1]([1]阪大院薬、[2]アスビオファーマ)、日本薬学会第130年会、平成22年3月、岡山

13. Claudin発現の迅速かつ簡便なモニタリングシステムの開発
渡利 彰浩、近藤 昌夫、八木 清仁(阪大院薬)、日本薬学会第130年会、平成22年3月、岡山

H. 知的財産権の出願・登録状況

H-1 特許取得

該当事項なし

H-2 実用新案登録

該当事項なし

H-3 その他

該当事項なし

I. 研究協力者

八木清仁(薬学研究科 教授)
渡利彰浩(薬学研究科 助教)
吉田孟史(薬学研究科 大学院生)
山本芙美(薬学研究科 大学院生)

研究成果の刊行に関する一覧表

書籍

著者氏名	論文タイトル名	書籍全体の編集者名	書 籍 名	出版社名	出版地	出版年	ページ
	該当事項なし						

雑誌

発表者氏名	論文タイトル名	発表誌名	巻号	ページ	出版年
Itoh A Isoda K Kondoh M Kawase M Kobayashi M Tamesada M Yagi K	Hepatoprotective effect of syringic acid and vanillic acid on concanavalin a-induced liver injury	*Biol. Pharm. Bull*	32	1215-1219	2009
Nishimori H Kondoh M Isoda K Tsunoda S Tsutsumi Y Yagi K	Histological analysis of 70-nm silica particles-induced chronic toxicity in mice	*Eur. J. Pharm. Biopharm.*	72	626-629	2009
Nishimori H Kondoh M Isoda K Tsunoda S Tsutsumi Y Yagi K	Silica nanoparticles as hepatotoxicants	*Eur. J. Pharm. Biopharm.*	72	496-501	2009
Nagano K Imai S Mukai Y Nakagawa S Abe Y Kamada H Tsunoda S Tsutsumi Y	Rapid isolation of intrabody candidates by using an optimized non-immune phage antibody library	*Pharmazie*	64	238-241	2009
Mukai Y Nakamura T Yoshioka Y Tsunoda S Kamada H Nakagawa S Yamagata Y Tsutsumi Y	Crystallization and preliminary X-ray analysis of TNF-TNFR2 complex	*Acta. Crystallogr*	65	295-298	2009

Mukai Y Nakamura T Yoshioka Y Shibata H Abe Y Nomura T Taniai M Ohta T Nakagawa S Tsunoda S Kamada H Yamagata Y Tsutsumi Y	Fast binding kinetics and conserved 3D structure underlie the antagonistic activity of mutant TNF: useful information for designing artificial proteo-antagonists	*J. Biochem.*	146	167-172	2009
Matsuhisa K Kondoh M Takahashi A Yagi K	Tight junction modulator and drug delivery	*Expert Opin Drug Deliv*	6	509-515	2009
Saeki R Kondoh M Kakutani H Tsunoda S Mochizuki Y Hamakubo T Tsutsumi Y Horiguchi Y Yagi K	A novel tumor-targeted therapy using a claudin-4-targeting molecule	*Mol Pharmacol*	76	918-926	2009
近藤昌夫 高橋梓 佐伯理恵 八木清仁	生体バリアを利用した創薬研究	*Drug Delivery System*	24	532-537	2009
Uchida H Kondoh M Hanada T Takahashi A Hamakubo T Yagi K	A claudin-4 modulator enhances the mucosal absorption of a biologically active peptide	*Biochem Pharmacol*	79	1437-1444	2010
Kakutani H Kondoh M Fukasaka M Suzuki H Hamakubo T Yagi K	Mucosal vaccination using claudin-4-targeting	*Biomaterials*			In press

Hepatoprotective Effect of Syringic Acid and Vanillic Acid on Concanavalin A-Induced Liver Injury

Ayano ITOH,[a] Katsuhiro ISODA,[a] Masuo KONDOH,[a] Masaya KAWASE,[a] Masakazu KOBAYASHI,[b] Makoto TAMESADA,[b] and Kiyohito YAGI*,[a]

[a] *Graduate School of Pharmaceutical Sciences, Osaka University; 1–6 Yamada-oka, Suita, Osaka 565–0871, Japan: and* [b] *Research and Development Center, Kobayashi Pharmaceutical Co., Ltd.; 1–30–3 Toyokawa, Ibaraki, Osaka 567–0057, Japan.* Received December 22, 2008; accepted March 18, 2009; published online April 17, 2009

The edible mushroom *Lentinula edodes* (shiitake) contains many bioactive compounds. In the present study, we cultivated *L. edodes* mycelia in solid medium and examined the hot-water extract (L.E.M.) for its suppressive effect on concanavalin A (ConA)-induced liver injury in mice. ConA injection into the tail vein caused a great increase in the serum aspartate aminotransferase (AST) and alanine aminotransferase (ALT) levels. The intraperitoneal administration of L.E.M. significantly decreased the levels of the transaminases. L.E.M. contains many bioactive substances, including polysaccharides and glucan, which could be immunomodulators. Since ConA-induced liver injury is caused by the activation of T cells, immunomodulating substances might be responsible for the suppressive effect of L.E.M. L.E.M. also contains phenolic compounds that are produced from lignocellulose by mycelia-derived enzymes. The major phenolics in L.E.M., syringic acid and vanillic acid, were intraperitoneally injected into mice shortly before the ConA treatment. Similar to L.E.M., the administration of syringic acid or vanillic acid significantly decreased the transaminase activity and suppressed the disorganization of the hepatic sinusoids. In addition, the inflammatory cytokines tumor necrosis factor (TNF)-α, interferon (IFN)-γ, and interleukin (IL)-6 in the serum increased rapidly, within 3 h of the ConA administration, but the administration of syringic acid or vanillic acid significantly suppressed the cytokine levels. Together, these findings indicate that the phenolic compounds in L.E.M. are hepatoprotective through their suppression of immune-mediated liver inflammation.

Key words hepatoprotection; *Lentinula edodes*; syringic acid; vanillic acid; concanavalin A

Many physiologically active hepatoprotective substances, such as those with antifibrotic activity, have been found in tea, fruits, and vegetables.[1,2] The edible mushroom *Lentinula edodes* (shiitake) contains several bioactive compounds, including compounds with immunoprotective and antiatherogenic activities and one compound with an anti-human immunodeficiency virus (HIV) effect.[3—5] The mycelia of *L. edodes* can be cultured in solid medium, and the extract obtained by hot-water treatment (L.E.M.) is commercially available as a nutritional supplement. In our previous study, we found that L.E.M. exerts a hepatoprotective effect on dimethylnitrosamine (DMN)-induced liver fibrosis and D-galactosamine-induced acute liver injury.[6,7] In the chronic liver injury model that uses DMN, the L.E.M. treatment suppressed the activation of hepatic stellate cells, which play a central role in liver fibrosis. The L.E.M. treatment also protected hepatocytes in the acute liver injury model that uses D-galactosamine. We also found that the oral or intraperitoneal administration of L.E.M. suppressed immune-mediated liver injury. Therefore, L.E.M. is a promising plant extract for the prevention of liver failure. With the aim of developing effective drugs for liver diseases, we examined the protective effect of a single L.E.M. component against liver injury.

The main components of L.E.M. are sugars, proteins, and polyphenolic compounds. The polyphenols act as antioxidants by scavenging reactive oxygen species (ROS), which produce oxidative stress and can adversely affect many cellular processes. Polyphenols have been proposed to protect against several diseases, including cancers, cardiovascular disease, and neurodegenerative disorders.[8—10] In our previous study, we found that the polyphenol-rich fraction of L.E.M. inhibits hepatic stellate cell activation, which is the main cause of liver fibrosis.[6] Among the polyphenols, syringic acid and vanillic acid are enriched in the solid medium of cultured *L. edodes* mycelia. *L. edodes* grown in lignocellulose secretes lignin-degrading peroxidase into the culture medium.[11] The mycelia-derived enzymes degrade the lignin to produce phenolic compounds, particularly syringic acid and vanillic acid. In the present study, we used a mouse model of liver injury to evaluate the hepatoprotective activity of these compounds.

Concanavalin A (ConA)-induced liver injury is a mouse model of immune-mediated liver injury that resembles viral and autoimmune hepatitis in humans.[12] The intravenous injection of ConA into mice increases the plasma alanine aminotransferase (ALT) level; simultaneously, activated T cells infiltrate the liver, and the apoptosis and necrosis of hepatocytes follows. The activation of T cells by ConA results in increased levels of inflammatory cytokines, including tumor necrosis factor (TNF)-α, interferon (IFN)-γ, and interleukin (IL)-6.[13] In the present study, we found that syringic acid and vanillic acid could suppress ConA-induced liver inflammation and damage in mice.

MATERIALS AND METHODS

Animals BALB/c mice were purchased from SLC (Shizuoka, Japan). The animals were housed in an air-conditioned room at 22 °C before the experiment. Hepatic injury was elicited in 6-week-old male mice by injecting ConA (20 mg/kg body weight) (Seikagaku Biobusiness, Tokyo, Japan) into the tail vein. L.E.M., syringic acid (WAKO, Osaka, Japan) or vanillic acid (WAKO, Osaka, Japan) was administered intraperitoneally just before the ConA adminis-

* To whom correspondence should be addressed. e-mail: yagi@phs.osaka-u.ac.jp

tration. L.E.M., syringic acid and vanillic acid were dissolved in sterilized phosphate buffered saline (PBS). Blood was collected from the orbital sinus 24 h after the ConA administration and analyzed for transaminases. The blood was sampled at 24 h because the transaminase levels peaked at 24 h after the ConA treatment. The animal experiments were conducted in accordance with the ethical guidelines of the Osaka University Graduate School of Pharmaceutical Sciences.

Analysis of Liver Enzymes The serum aspartate aminotransferase (AST) and ALT levels were measured by using an assay kit (Transaminase C, WAKO, Osaka, Japan).

Cytokine Determination by ELISA The IL-6, TNF-α, and IFN-γ levels in serum samples were determined by using a mouse enzyme-linked immunosorbent assay (ELISA) kit (Biosource, San Jose, CA, U.S.A.). Analyses were performed according to the manufacturer's instructions. The blood samples were collected at 3, 6, and 9 h because the cytokine levels increased more rapidly than the transaminases and returned to almost normal levels within 12 h.

Histological Analysis Liver specimens were fixed in 4% paraformaldehyde and embedded in paraffin. The tissue blocks were cut into 3-μm sections that were mounted on slides and stained with hematoxylin–eosin.

DPPH Radical-Scavenging Activity The free radical-scavenging activities of L.E.M., syringic acid, and vanillic acid were measured by using the 1,1-diphenyl-2-picrylhdrazyl (DPPH) method.[14] DPPH is a stable free radical that was used for evaluating the scavenging activity by end-point assay. Each compound at the concentration of 0.01 to 1.0 mg/ml was dissolved in ethanol and mixed with DPPH. The reaction was completed within a few minutes. After a 20-min incubation at room temperature in the dark, the absorbance of the sample was read at 517 nm by using a spectrophotometer. The scavenging activity was shown by the decrease in the absorbance at 517 nm.

Preparation of L.E.M. L.E.M. was prepared as previously reported.[15] Briefly, *L. edodes* mycelia were cultivated in solid medium composed of sugarcane bagasse and defatted rice bran. To prepare the culture extract, hot water was added to the medium including the mycelia, and the extract was filtered and lyophilized before being used as the L.E.M. preparation.

Statistics The data were analyzed for statistical significance by the non-parametric Steel–Dwass multiple comparison method. p values less than 0.05 were considered statistically significant.

RESULTS

Effect of L.E.M. on ConA-Induced Liver Injury We examined the hepatoprotective effect of L.E.M. on ConA-induced liver injury in mice. Various amounts of L.E.M. were injected intraperitoneally just before the ConA injection. Twenty-four hours after ConA treatment, the activities of serum AST and ALT were greatly increased as compared to the untreated control (Fig. 1). The intraperitoneal administration of L.E.M. at 20 mg/kg body weight significantly decreased the AST and ALT levels. When administered orally 2 weeks before the ConA treatment, L.E.M. significantly suppressed the increase in transaminases (data not shown).

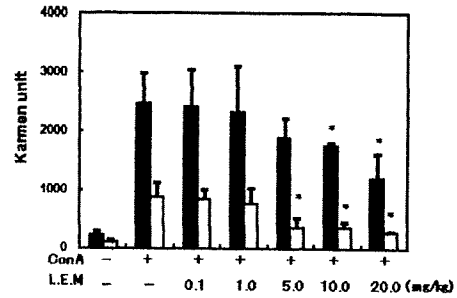

Fig. 1. Effect of L.E.M. on ConA-Induced Liver Injury

Mice received an intravenous injection of ConA (20 mg/kg) and an intraperitoneal injection of L.E.M. (0.1—20 mg/kg). Blood was collected to determine the serum levels of AST (solid columns) and ALT (open columns). The values are the means ± S.D. (n=4). *p<0.05 as compared to ConA treatment alone.

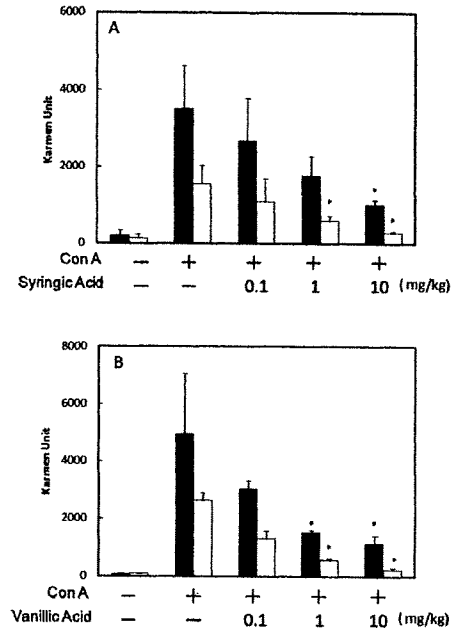

Fig. 2. Effect of Syringic Acid or Vanillic Acid on Transaminase Leakage in ConA-Induced Liver Injury in Mice

Syringic acid (A) or vanillic acid (B) was injected intraperitoneally shortly before the intravenous injection of ConA (20 mg/kg). Blood was collected to measure the serum levels of AST (solid columns) and ALT (open columns). Values are the means±S.D. (n=4). *p<0.05 as compared to the ConA treatment alone.

These results indicate that L.E.M. has a protective effect against ConA-induced liver injury.

Effect of Syringic and Vanillic Acid on ConA-Induced Liver Injury We next examined the hepatoprotective effect of syringic and vanillic acid on the ConA-induced liver injury in mice. Syringic or vanillic acid (0.1, 1.0, or 10.0 mg/kg body weight) was injected intraperitoneally just before the ConA injection. The intraperitoneal administration of syringic or vanillic acid dose-dependently decreased the activities of AST and ALT (Fig. 2). To obtain histological evidence for the protection from liver injury, liver sections were prepared and stained with hematoxylin and eosin; representative images are shown in Fig. 3. The structure of the hepatic sinusoids was normal in the sections from untreated mice. In contrast, the hepatic sinusoids were disorganized and inflammatory infiltration was present in the liver sections from the ConA-treated mice, showing that the liver was injured by the tail-vein injection of ConA. Although some hepatocytes

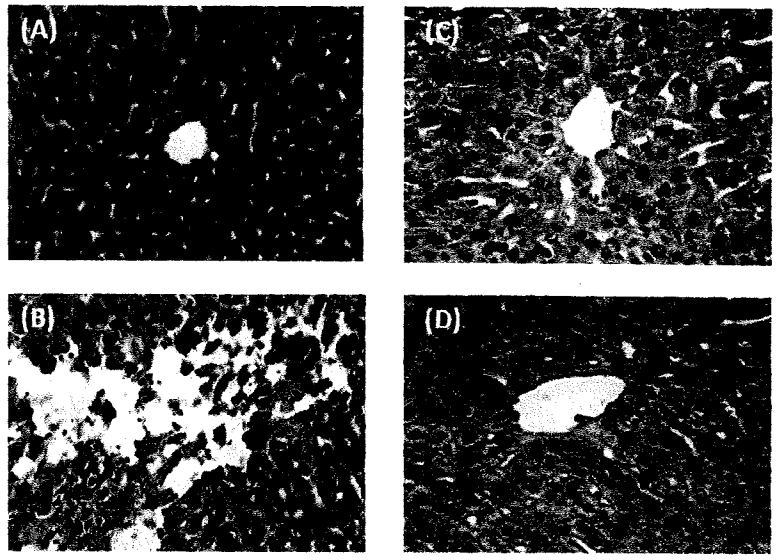

Fig. 3. Suppression of ConA-Induced Liver Injury in Mice That Received Syringic Acid or Vanillic Acid

Sections of paraffin-embedded liver tissue were stained with hematoxylin–eosin. The liver was excised from normal (A), ConA-injured control (B), syringic acid-treated (C), and vanillic acid-treated (D) mice 24 h after ConA injection. Magnification for all photographs, ×400.

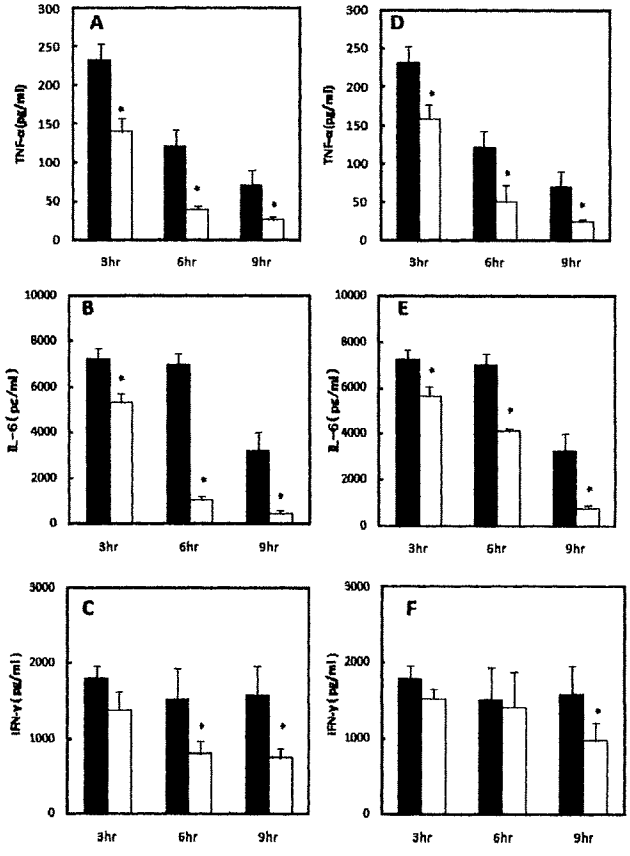

Fig. 4. Changes in Serum TNF-α (A, D), IL-6 (B, E), and IFN-γ (C, F) Levels Measured by ELISA

Mice received an intravenous injection of ConA and intraperitoneal injection of syringic acid (A, B, C) or vanillic acid (D, E, F). Cytokine levels were measured 3, 6, and 9 h after ConA treatment. Solid and open columns indicate the ConA treatment alone and the phenolics treatment, respectively. Values are the means±S.D. (n=4). *p<0.05 as compared to the ConA treatment alone.

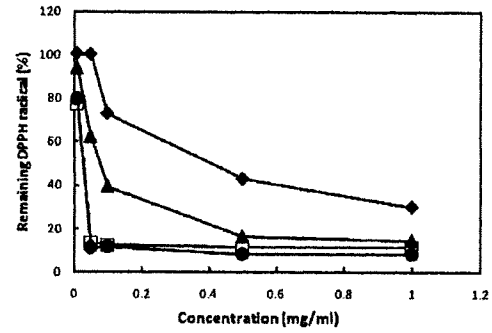

Fig. 5. DPPH Radical-Scavenging Activity of L.E.M., Syringic Acid, and Vanillic Acid

The amount of DPPH radicals was spectrophotometrically determined at 517 nm. Various concentrations of L.E.M. (diamond), syringic acid (open square), and vanillic acid (triangle) were tested. Ascorbic acid (circle) was used as a positive control. Values are the means ' S.D. (n 3).

lacking nuclei were seen around the vessel, the disorganization caused by the ConA treatment was decreased in the sections from mice treated with 10 mg/kg of syringic acid or vanillic acid (Figs. 3C, D). Next, we measured the TNF-α, IFN-γ, and IL-6 levels in serum 3, 6, and 9 h after ConA treatment (Fig. 4). The intraperitoneal injection of 10 mg/kg of syringic or vanillic acid significantly decreased the cytokine levels in the serum. These results clearly indicate that syringic acid and vanillic acid have a protective effect against ConA-induced liver injury.

DPPH Radical-Scavenging Activity of L.E.M., Syringic Acid, and Vanillic Acid Figure 5 shows the radical scavenging activities of the samples with DPPH as the substrate. L.E.M. had a dose-dependent scavenging activity that was probably derived from the phenolic compounds including syringic acid and vanillic acid. Both syringic acid and vanillic acid had DPPH radical-scavenging activity; syringic acid had a much higher activity than vanillic acid. This anti-oxidation activity could potentially be effective for suppressing oxidative stress-derived liver injury.

DISCUSSION

This study showed that L.E.M., the hot water extract of cultured mycelia, had a hepatoprotective effect against ConA-induced liver injury in mice, a widely used model of viral hepatitis. Since ConA-induced liver injury is caused by the activation of T cells, the potential immunomodulators contained in the L.E.M., including polysaccharides, glucans, and eritadenine[4,16] could be responsible for the suppressive effect of L.E.M. L.E.M. also contains phenolic compounds that have antioxidation activity, and we previously reported that the administration of L.E.M. suppresses oxidative stress-induced liver injury.[6,7] In the present study, we found that the anti-oxidative phenolic compounds syringic acid and vanillic acid strongly suppressed ConA-induced liver injury in mice.

The physiological functions of plant-derived phenolic compounds have been previously described. Syringic and vanillic acid are reported to possess antimicrobial, anti-cancer, and anti-DNA oxidation activities.[17—19] The present study provides the first evidence that both of these compounds suppress transaminase leakage and inflammatory cytokine production in mice that have ConA-induced liver injury. When these phenolics are orally administered to hamsters, they are absorbed and appear in the plasma within 40 min.[20] Thus, although the phenolics were injected intraperitoneally in the present study, oral administration might also elicit a positive effect on liver injury. Furthermore, these compounds can be obtained in large amounts from inexpensive sources, such as sugarcane molasses. Therefore, syringic and vanillic acid might be promising internal medicines or supplements for suppressing the effects of immune-mediated liver injury, such as the persistent inflammation caused by hepatitis virus infection.

Syringic acid and vanillic acid significantly suppressed the increase in the inflammatory cytokines TNF-α, IFN-γ, and IL-6 elicited *in vivo* by the T-cell mitogen, ConA. Therefore, phenolics might alleviate the uncontrolled immune response through immunomodulation. Sharma *et al.* reported that the plant-derived antioxidant, chlorophyllin, inhibits ConA-induced lymphocyte proliferation *in vitro*.[21] Another antioxidant, resveratrol, is reported to inhibit the production of cytokines, such as IFN-γ and TNF-α, in ConA-treated spleen cells and macrophages.[22] Although chlorophyllin and resveratrol possess various activities that could be responsible for these results, their antioxidation activity could be a major contributor to the suppression of lymphocyte activation. Pani reported that the proliferation of mouse thymocytes in response to ConA treatment is strongly inhibited by the ROS scavenger, *N*-acetylcysteine, and by the inhibitor of NADPH oxidase, diphenyleneiodonium.[23] NADPH oxidase generates ROS after its activation in cells by various types of stimulation.[24] Therefore, the suppressive effect of syringic and vanillic acid on the ConA-induced liver injury might be due to their scavenging of ROS generated by activated NADPH oxidase in the lymphocytes. ConA induces a massive recruitment of activated T cells to the liver. Schwabe reported that ConA-induced liver injury is largely dependent on membrane-bound TNF-α on the infiltrating T cells. The TNF binds to its receptor on hepatocytes to induce ROS production.[24] Syringic acid and vanillic acid could scavenge the ROS to suppress hepatocyte death.

Although syringic and vanillic acids had almost the same effect on liver protection, syringic acid had stronger DPPH activity than vanillic acid. There might be alternative characteristic of these phenolic compounds that are responsible for their liver-protecting effect. Caffeic acid phenethyl ester (CAPE), which is an active phenolic compound contained in propolis, has immunomodulatory and anti-inflammatory properties.[25] Since DNA-binding and transcriptional activities of NF-κB are inhibited in CAPE-treated Jurkat cells, CAPE appears to suppress the proliferation of T cells. Curcumin, a phenolic compound with various biological activities including immunomodulation, suppressed TNF-induced NF-κB-dependent gene transcription.[26] Curcumin and CAPE covalently modify sulfhydryl groups by oxidation and alkylation, and the modification might be responsible for the inhibition of the NF-κB-dependent process. Syringic acid, vanillic acid, and curcumin are phenolic compounds that possess *O*-methoxy groups. Therefore, it is possible that the immunomodulatory effect of syringic and vanillic acids is mediated by inhibiting the NF-κB-dependent process. In the present study, we showed that the cytokine levels were lowered after the administration of syringic acid or vanillic acid in ConA-treated mice; however, the level of suppression was smaller than the anti-inflammatory effect. The inhibition of TNF-induced NF-κB-dependent processes might play an important role in protection against ConA-induced liver injury.

In addition to the ConA-induced acute liver injury, we found that syringic and vanillic acid extensively suppressed the liver fibrosis elicited by chronic treatment with carbon tetrachloride (to be published elsewhere). Thus, these phenolics appear to have physiologically versatile functions. Further studies on the bioavailability, toxicity, and stability of these compounds are underway. The contents of syringic acid and vanillic acid in L.E.M. are 450 and 378 μg/g, respectively. Thus, the contents are relatively small, and the phenolics might not play a major role in immunomodulation effect of L.E.M. However, these phenolics are small molecules that can be easily synthesized in large amounts by organic reactions. These characteristics have clear advantages over immunomodulating glucan or polysaccharide, which seem to be the major components in L.E.M. for drug development.

Acknowledgements We thank the members of our laboratory for their useful comments and discussion.

REFERENCES

1) Gebhardt R., *Planta Med.*, **68**, 289—296 (2002).
2) McKillop I. H., Schrum L. W., *Alcohol*, **35**, 195—203 (2005).
3) Suzuki H., Okubo A., Yamazaki S., Suzuki K., Mitsuya H., Toda S., *Biochem. Biophys. Res. Commun.*, **160**, 367—373 (1989).
4) Yamada T., Oinuma T., Niihashi M., Mitsumata M., Fujioka T., Hasegawa K., Nagaoka H., Itakura H., *J. Atheroscler. Thromb.*, **9**, 149—156 (2002).
5) Yamamoto Y., Shirono H., Kono K., Ohashi Y., *Biosci. Biotechnol. Biochem.*, **61**, 1909—1912 (1997).
6) Akamatsu S., Watanabe A., Tamesada M., Nakamura R., Hayashi S., Kodama D., Kawase M., Yagi K., *Biol. Pharm. Bull.*, **27**, 1957—1960 (2004).
7) Watanabe A., Kobayashi M., Hayashi S., Kodama D., Isoda K., Kondoh M., Kawase M., Tamesada M., Yagi K., *Biol. Pharm. Bull.*, **29**, 1651—1654 (2006).
8) Aggarwal B. B., Kumar A., Bharti A. C., *Anticancer Res.*, **23**, 363—398 (2003).

9) Aviram M., Dornfeld L., Kaplan M., Coleman R., Gaitini D., Nitecki S., Hofman A., Rosenblat M., Volkova N., Presser D., Attias J., Hayek T., Fuhrman B., *Drugs Exp. Clin. Res.*, **28**, 49—62 (2002).
10) Levites Y., Weinreb O., Maor G., Youdim M. B., Mandel S., *J. Neurochem.*, **78**, 1073—1082 (2001).
11) Forrester I. T., Grabski A. C., Mishra C., Kelley B. D., Strickland W. N., Leatham G. F., Burgess R. R., *Appl. Microbiol. Biotechnol.*, **33**, 359—365 (1990).
12) Tiegs G., Hentschel J., Wendel A., *J. Clin. Invest.*, **90**, 196—203 (1992).
13) Cao Q., Batey R., Pang G., Russell A., Clancy R., *Immunol. Cell Biol.*, **76**, 542—549 (1998).
14) Velazquez C., Navarro M., Acosta A., Angulo A., Dominguez Z., Robles R., Robles Zepeda R., Lugo E., Goycoolea F. M., Velazquez E. F., Astiazaran H., Hernandez J., *J. Appl. Microbiol.*, **103**, 1747—1756 (2007).
15) Mizoguchi Y., Katoh H., Kobayashi K., Yamamoto S., Morisawa S., *Gastroenterol. Jpn.*, **22**, 459—464 (1987).
16) Wasser S. P., Weis A. L., *Crit. Rev. Immunol.*, **19**, 65—96 (1999).
17) Aziz N. H., Farag S. E., Mousa L. A., Abo Zaid M. A., *Microbios*, **93**, 43—54 (1998).
18) Guimaraes C. M., Giao M. S., Martinez S. S., Pintado A. I., Pintado M. E., Bento L. S., Malcata F. X., *J. Food Sci.*, **72**, C039—C043 (2007).
19) Kampa M., Alexaki V. I., Notas G., Nifli A. P., Nistikaki A., Hatzoglou A., Bakogeorgou E., Kouimtzoglou E., Blekas G., Boskou D., Gravanis A., Castanas E., *Breast Cancer Res.*, **6**, R63—R74 (2004).
20) Chen C. Y., Milbury P. E., Kwak H. K., Collins F. W., Samuel P., Blumberg J. B., *J. Nutr.*, **134**, 1459—1466 (2004).
21) Sharma D., Kumar S. S., Sainis K. B., *Mol. Immunol.*, **44**, 347—359 (2007).
22) Gao X., Xu Y. X., Janakiraman N., Chapman R. A., Gautam S. C., *Biochem. Pharmacol.*, **62**, 1299—1308 (2001).
23) Pani G., Colavitti R., Borrello S., Galeotti T., *Biochem. J.*, **347 Pt 1**, 173—181 (2000).
24) Bedard K., Krause K. H., *Physiol. Rev.*, **87**, 245—313 (2007).
25) Marquez N., Sancho R., Macho A., Calzado M. A., Fiebich B. L., Munoz E., *J. Pharmacol. Exp. Ther.*, **308**, 993—1001 (2004).
26) Aggarwal S., Ichikawa H., Takada Y., Sandur S. K., Shishodia S., Aggarwal B. B., *Mol. Pharmacol.*, **69**, 195—206 (2006).

European Journal of Pharmaceutics and Biopharmaceutics xxx (2009) xxx–xxx

Contents lists available at ScienceDirect

European Journal of Pharmaceutics and Biopharmaceutics

journal homepage: www.elsevier.com/locate/ejpb

Research paper

Silica nanoparticles as hepatotoxicants

Hikaru Nishimori [a], Masuo Kondoh [a,*], Katsuhiro Isoda [a], Shin-ichi Tsunoda [b,c], Yasuo Tsutsumi [b,c,d], Kiyohito Yagi [a]

[a] Laboratory of Bio-Functional Molecular Chemistry, Graduate School of Pharmaceutical Sciences, Osaka University, Osaka, Japan
[b] Laboratory of Pharmaceutical Proteomics, National Institute of Biomedical Innovation, Osaka, Japan
[c] The Center for Advanced Medicinal Engineering and Informatics, Osaka University, Osaka, Japan
[d] Laboratory of Toxicology, Graduate School of Pharmaceutical Sciences, Osaka University, Osaka, Japan

ARTICLE INFO

Article history:
Received 16 October 2008
Accepted in revised form 9 February 2009
Available online xxxx

Keywords:
Silica particle
Nano-size particle
Liver injury

ABSTRACT

Nano-size materials are increasingly used in cosmetics, diagnosis, imaging and drug delivery, but the toxicity of the nano-size materials has never been fully investigated. Here, we investigated the relationship between particle size and toxicity using silica particles with diameters of 70, 300 and 1000 nm (SP70, SP300, and SP1000) as a model material. To evaluate acute toxicity, we first performed histological analysis of liver, spleen, kidney and lung by intravenous administration of silica particles. SP70-induced liver injury at 30 mg/kg body weight, while SP300 or 1000 had no effect even at 100 mg/kg. Administration of SP70 dose-dependently increased serum markers of liver injury, serum aminotransferase and inflammatory cytokines. Repeated administration of SP70 twice a week for 4 weeks, even at 10 mg/kg, caused hepatic fibrosis. Taken together, nano-size materials may be hepatotoxic, and these findings will be useful for future development in nanotechnology-based drug delivery system.

1. Introduction

The recent development of technology for reducing material size has provided innovative nanomaterials. Nanomaterials are engineered structures with at least one dimension of 100 nm or less, and have unique physicochemical properties with regard to size, chemical composition, surface structure, solubility, shape and aggregation. Nanomaterials have been widely used in microelectronics, catalysts, ultra-sensitive molecular sensing and imaging probes, pharmaceutical agents and cosmetics. Thus, the development of reduced particle size from the macro to the nanoscale provides benefits to a range of industrial and scientific fields. However, materials that are inert in bulk form may be toxic in nano-size forms, and it is thus essential to understand the biological activities and potential toxicity of nanomaterials [1–3].

The influence of inhalation of nanomaterials on human health has been widely investigated. Occupational exposure to quartz, mineral dust particles and asbestos induce inflammation, fibrosis and cytotoxicity in the lung [3]. In animal models, inhaled nanoparticles do not locally remain in the lung, and pass into blood flow, resulting in distribution to distant organs, such as the liver, kidney, brain and heart [4–7]. Moreover, biomedical applications for diagnosis and therapeutic purposes will require intravenous, subcutaneous or intramuscular administration [8–10]. Thus, it is necessary to confirm the influence of nanomaterials in systemic flow on various organs.

Silica nanoparticles have been applied to diagnosis and drug delivery [4,11], and intraperitoneal administration of silica nanoparticles results in the biodistribution of the nanoparticles to diverse organs, such as the liver, kidney, spleen and lung [4]. Both micro- and nano-size silica particles are also commercially available. In the present study, we investigated the influence of nanomaterials on major organs, such as the liver, kidney, spleen and lung using silica particles as a model material. When silica particles with a diameter of 70, 300 or 1000 nm were intravenously injected, only the 70-nm particles led to acute and chronic liver injury.

2. Materials and methods

2.1. Materials

Silica nanoparticles with a diameter of 70, 300 or 1000 nm were purchased from Micromod Partikeltechnologie GmbH (Rostock,

Abbreviations: SP70, 70 nm silica particles; SP300, 300 nm silica particles; SP1000, 1000 nm silica particles; ALT, aminotransferase; BUN, blood urea nitrogen; IL-6, interleukin-6; TNF-α, tumor necrosis factor-α; $GdCl_3$, gadolinium chloride; CPA, cyclophosphamide; LSEC, liver sinusoidal endothelial cells; MARCO, macrophage receptor with collagenous structure.

* Corresponding author. Laboratory of Bio-Functional Molecular Chemistry, Graduate School of Pharmaceutical Sciences, Osaka University, Suita, Osaka 5650871, Japan. Tel.: +81 6 6879 8196; fax: +81 6 6879 8199.
E-mail address: masuo@phs.osaka-u.ac.jp (M. Kondoh).

0939-6411/$ - see front matter © 2009 Elsevier B.V. All rights reserved.
doi:10.1016/j.ejpb.2009.02.005

Please cite this article in press as: H. Nishimori et al., Silica nanoparticles as hepatotoxicants, Eur. J. Pharm. Biopharm. (2009), doi:10.1016/j.ejpb.2009.02.005

Germany). The average size of the silica particles was determined to be 75.7, 311 and 830 nm by Zetasizer (Sysmex Co., Kobe, Japan). The particles were spherical and nonporous. The particles were stocked at 25 mg/ml (70 nm) and 50 mg/ml (300 and 1000 nm) in aqueous suspension. The stock solutions were suspended using vortex mixer for 5 min before use. The resultant solutions did not show aggregation of the particles by electron microscopy analysis. Reagents used in this study were of research grade.

2.2. Animals

BALB/c male mice (8 wk) were obtained from Shimizu Laboratory Supplies Co., Ltd. (Kyoto, Japan), and were housed in an environmentally controlled room at 23 ± 1.5 °C with a 12-h light/12-h dark cycle. Mice had free access to water and commercial chow (Type MF, Oriental Yeast, Tokyo, Japan). Mice were intravenously injected with the silica particles at 10–100 mg/kg body weight. The experimental protocols conformed to the ethical guidelines of the Graduate School of Pharmaceutical Sciences, Osaka University.

2.3. Histological analysis

The liver, kidney, spleen and lung were removed and fixed with 4% paraformaldehyde. After sectioning, thin tissue sections of tissues were stained with hematoxylin and eosin for histological observation. Liver sections were stained with Azan-Mallory for observation of liver fibrosis.

2.4. Biochemical assay

Serum alanine aminotransferase (ALT) levels and blood urea nitrogen (BUN) were measured using a commercially available Transaminase-CII kit and Blood Urea Nitrogen-B Test Wako (WAKO Pure Chemical, Osaka, Japan), respectively. Interleukin-6 (IL-6) and tumor necrosis factor-α (TNF-α) were measured with an ELISA kit (BioSource International, CA, USA).

2.5. Gadolinium chloride assay

For Kupffer cell blockage of phagocytosis and partial depletion in the liver, mice were injected intravenously with gadolinium chloride ($GdCl_3$) at 10 mg/kg body weight at 30 and 6 h prior to intravenous administration of nanoparticles [12,13]. Blood was then recovered 24 h after injection of nanoparticles for ALT assay.

2.6. Cyclophosphamide assay

Disruption of liver sinusoidal endothelial cells was carried out by intraperitoneal injection of 300 mg/kg body weight cyclophosphamide (CPA) at 24 h prior to administration of nanoparticles [14,15]. Blood was recovered at 24 h after injection of nanoparticles for ALT assay.

2.7. Hepatic hydroxyproline content

Hepatic hydroxyproline content was assayed by Kivirikko's method, with some modification [16]. Briefly, liver tissue was hydrolyzed in 6 M HCl at 110 °C for 24 h in a glass tube. After centrifugation, the resultant supernatant was neutralized with 8 N KOH, and 2 g of KCl and 1 ml of 0.5 M borate buffer were then added, followed by incubation for 15 min at room temperature and further incubation for 15 min at 0 °C. Chloramine-T solution was then prepared and added. After additional incubation for 1 h at 0 °C, 2 ml of 3.6 M sodium thiosulfate was added, followed by incubation at 120 °C for 30 min. Next, 3 ml of toluene was added with incubation for a further 20 min at room temperature. After centrifugation, 2 ml of the resultant supernatant was added to Ehrlich's reagent, followed by incubation for 30 min at room temperature. Subsequently, the absorbance was measured at 560 nm.

2.8. Statistical analysis

Statistical analysis was performed by two-way ANOVA, followed by Student's *t*-test. The level of significance was set at $p < 0.05$.

3. Results

3.1. Liver injury by 70-nm silica nanoparticles

We initially investigated the acute toxicity of silica particles with diameters of 70 (SP70), 300 (SP300) or 1000 nm (SP1000) at maximal dose of 100 mg/kg. Intravenous injection of SP70 at 50 and 100 mg/kg was often lethal, but mice injected with SP300 and SP1000 survived. Fig. 1 shows hematoxylin–eosin staining of the liver, spleen, lung and kidney in silica particle-injected mice. We found no toxicity in any of these organs in SP300 or SP1000-injected mice at 100 mg/kg, and we found no abnormalities in the spleen, kidney and lung in SP70-injected mice at 30 mg/kg (Fig. 1A–D). However, degenerative necrosis of hepatocytes in the liver was observed in SP70-injected mice, thus suggesting that SP70 is toxic to the liver (Fig. 1A).

Next, in order to confirm the hepatotoxicity of SP70, we examined serum ALT activity, a biochemical marker of liver injury. Consistent with the histological data, injection of SP70 elevated serum ALT levels 35-fold over control values at 30 mg/kg, but injection of SP300 or SP1000 had no effect even at 100 mg/kg (Fig. 2A). Elevation of blood urea nitrogen, a biochemical marker of kidney injury, was not observed (Fig. 2B). Serum levels of inflammatory cytokine IL-6 and TNF-α were markedly elevated to 1124 and 80 pg/ml, respectively, in SP70-treated mice at 3 h (Fig. 2B and C). Slight elevation of serum IL-6 levels was observed in SP300- and SP1000-injected mice (28 and 32 pg/ml, respectively), while no elevation of TNF-α was observed. The IL-6 levels seen in SP300- or SP1000-treated mice were insufficient for liver injury. To investigate dose dependency of SP70-induced liver injury, we also investigated serum ALT and inflammatory cytokine levels at 12 h after SP70 administration. ALT, IL-6 and TNF-α levels were elevated in a dose-dependent manner after SP70 injection, and significant increases were observed with doses as low as 20 mg/kg (Fig. 3A–C). Taken together, these data suggest that 70-nm silica particles are toxic to the liver.

3.2. Involvement of Kupffer cells in SP70-induced liver injury

Kupffer cells are large liver macrophages, and are localized within the liver sinusoidal cells. Kupffer cells play a role in defense against various particles and substances entering the liver through the portal circulation [17]. Indeed, Kupffer cells clear virus particles from the bloodstream by phagocytosis [18–20]. The phagocytosis of parasites by Kupffer cells is accompanied by the release of pro-inflammatory cytokines that act as a paracrine signal to neighboring hepatocytes, and induce chemotaxis and aggregation of neutrophils. $GdCl_3$ inhibits phagocytosis by Kupffer cells and transiently eliminates Kupffer cells [12], and $GdCl_3$ has thus been widely used to investigate the roles of Kupffer cells in the liver [21,22]. To investigate the involvement of Kupffer cells in particle-induced liver injury, we evaluated the effects of $GdCl_3$ on nanoparticle-induced liver injury. As shown in Fig. 4A, pre-injection of $GdCl_3$ prior to injection of SP70 elevated serum ALT levels 5.5-fold

Please cite this article in press as: H. Nishimori et al., Silica nanoparticles as hepatotoxicants, Eur. J. Pharm. Biopharm. (2009), doi:10.1016/j.ejpb.2009.02.005

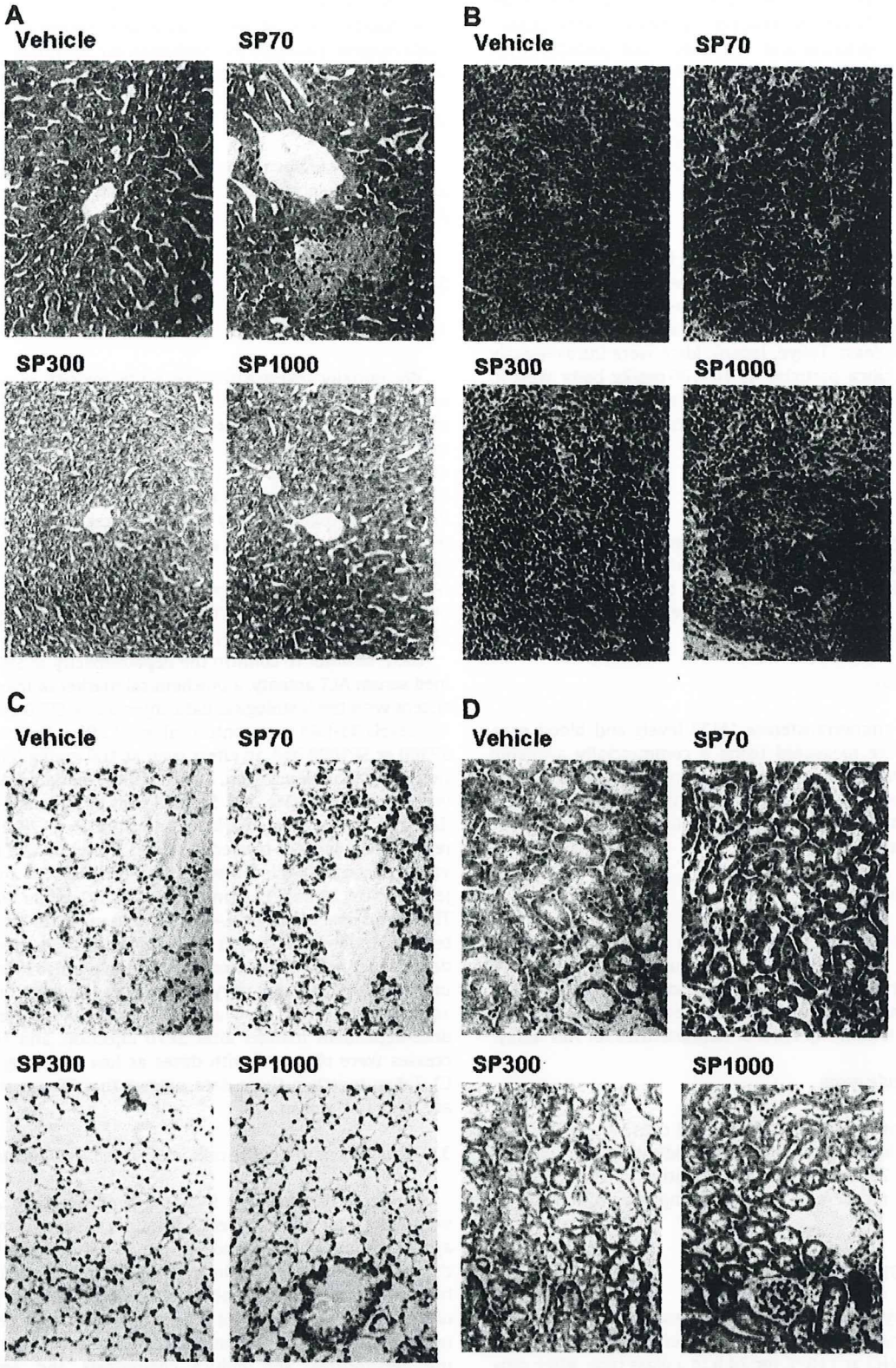

Fig. 1. Histological analysis of tissues in silica particle-treated mice. Silica particles with diameters of 70 (SP70), 300 (SP300) or 1000 nm (SP1000) were intravenously administered to mice at 30, 100 and 100 mg/kg, respectively. At 24 h after administration, tissues of liver (A), spleen (B), lung (C) and kidney (D) were collected, and fixed with 4% paraformaldehyde. Tissue sections were stained with hematoxylin and eosin and observed under a microscope. Data are representative of at least four mice.

in the SP70-injected group. In contrast, pre-injection of $GdCl_3$ did not affect ALT levels in the SP300- or SP1000-administered group. Taken together, these results indicate that phagocytosis of SP70 by Kupffer cells may attenuate liver injury, but the release of proinflammatory cytokines from Kupffer cells is not associated with SP70-induced liver injury.

Please cite this article in press as: H. Nishimori et al., Silica nanoparticles as hepatotoxicants, Eur. J. Pharm. Biopharm. (2009), doi:10.1016/j.ejpb.2009.02.005

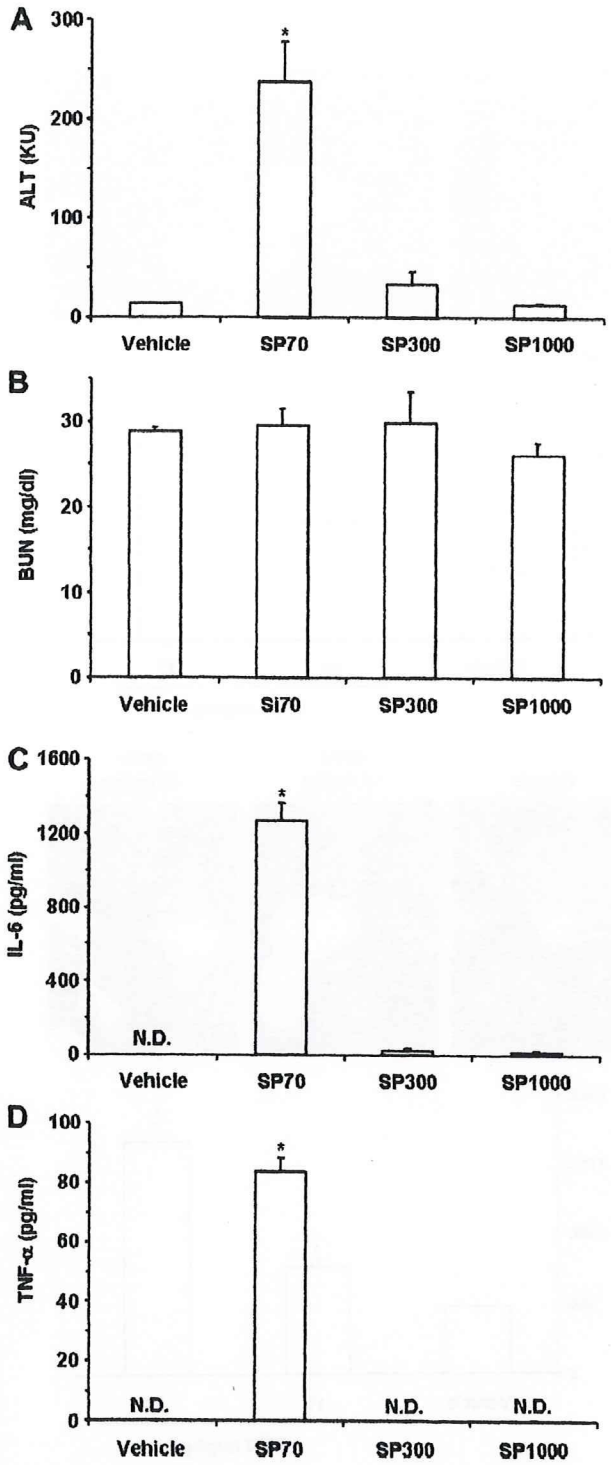

Fig. 2. Biochemical analyses of liver injury in silica particle-injected mice. SP70, SP300 or SP1000 was intravenously injected to mice at 30, 100 or 100 mg/kg, respectively. Blood was recovered at 3 and 24 h of the injection. Serum ALT (A) and BUN (B) at 24 h and IL-6 (C) and TNF-α (D) levels at 3 h were measured using a commercially available kit, as described in Section 2. Data are means ± SEM ($n = 4$). *Significant difference vs. vehicle-treated group ($p < 0.05$).

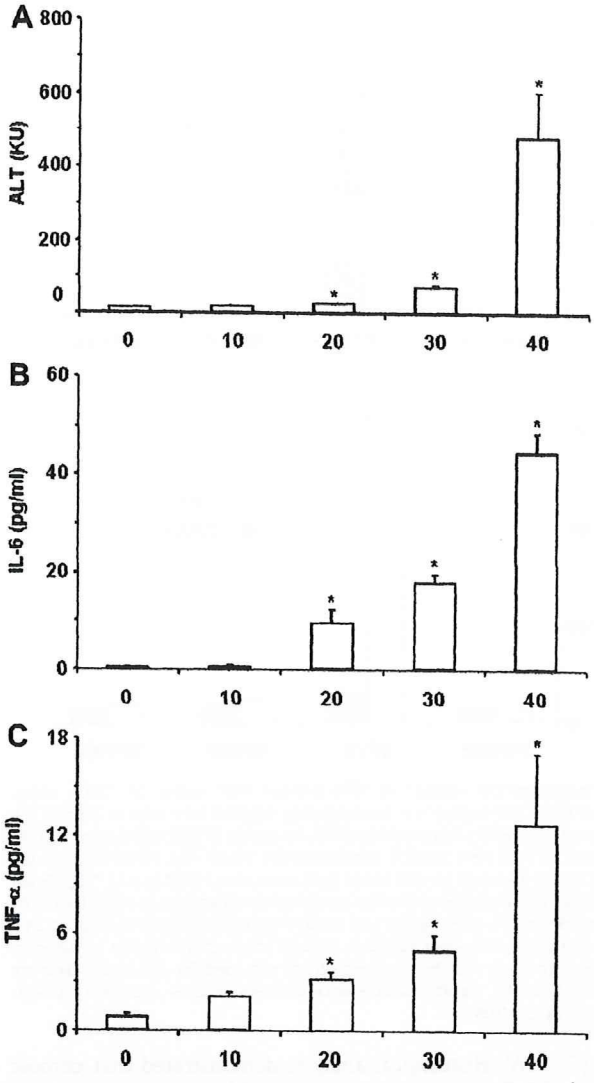

Fig. 3. Dose dependency of SP70 on liver injury. SP70 were intravenously administered at the indicated doses, and blood was recovered at 12 h after administration. Serum was used for measurement of ALT (A), IL-6 (B) and TNF-α (C), as described in Section 2. Data are means ± SEM ($n = 4$). *Significant difference compared with the vehicle-treated group ($p < 0.05$).

3.3. Involvement of liver sinusoidal endothelial cells in SP70-induced liver injury

Sinusoidal endothelium forms a barrier between the bloodstream and hepatocytes, preventing passage of particles. Liver sinusoidal endothelial cells (LSECs) are perforated by fenestrations, which are pores of approximately 100 nm in diameter. SP70, but not SP300 and SP1000, may pass through LSECs to the hepatocytes, resulting in liver injury. To evaluate this hypothesis, we performed CPA assay. CPA is converted in the liver to toxic metabolites, 4-hydroperoxycyclophosphamide and acrolein, to which endothelial cells are 20-fold more susceptible than hepatocytes [14]. CPA has been shown to disrupt LSECs [14,15]. We thus investigated the effects of CPA on nanoparticle-induced liver injury. As shown in Fig. 4B, pre-injection of CPA did not affect ALT levels in SP300- or SP1000-administered mice, whereas CPA dramatically decreased ALT levels to near control values in SP70-injected mice (from 235 to 29 KU). These data on CPA indicate that LSECs may be directly or indirectly involved in SP70-induced liver injury, but may not be a barrier against SP70.

3.4. Chronic toxicity of SP70

Finally, we investigated the effects of SP70 on chronic liver injury. SP70 was injected into mice every 3 days for 4 weeks at 10 or 30 mg/kg. The lower dose (10 mg/kg) did not cause acute liver

Please cite this article in press as: H. Nishimori et al., Silica nanoparticles as hepatotoxicants, Eur. J. Pharm. Biopharm. (2009), doi:10.1016/j.ejpb.2009.02.005

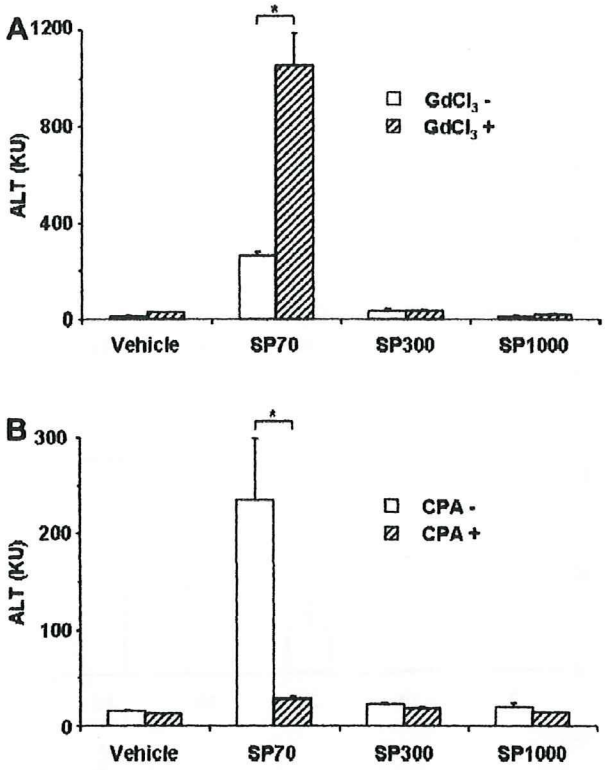

Fig. 4. Pharmaceutical analysis of SP70-induced liver injury. (A) $GdCl_3$ assay. Vehicle or $GdCl_3$ (10 mg/kg) was intravenously injected into mice at 30 h or 6 h prior to treatment with silica particles (SP70, 30 mg/kg; SP300, 100 mg/kg; SP1000, 100 mg/kg). At 24 h after particle administration, blood was recovered, and the resultant serum was used for ALT assay. Data are means ± SEM ($n = 4$). *Significant difference between vehicle- and silica particle-treated groups ($p < 0.05$). (B) CPA assay. Vehicle or CPA (300 mg/kg) was intraperitoneally injected to mice at 24 h prior to treatment with silica particles. At 24 h after administration of particles, blood was recovered, and the resultant serum was used for ALT assay. Data are means ± SEM ($n = 4$). *Significant difference between vehicle- and silica particle-treated groups ($p < 0.05$).

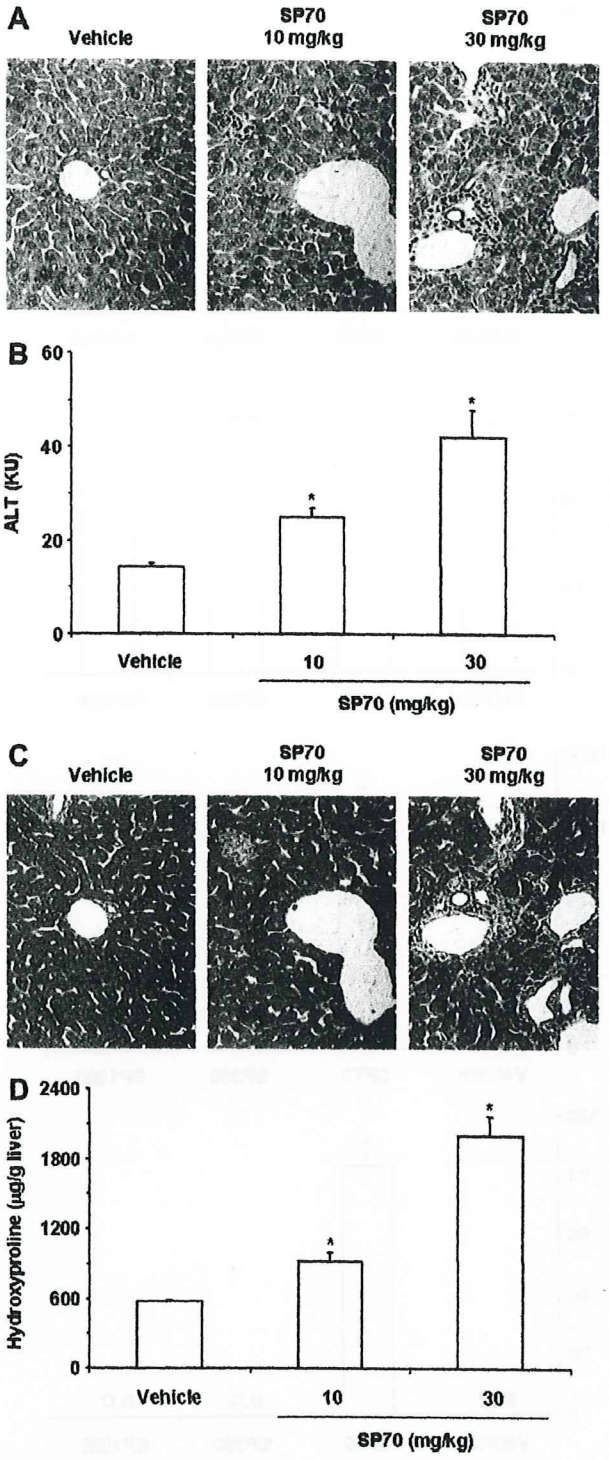

Fig. 5. Effect of SP70 on chronic liver injury. Mice were subjected to repeated administration of SP70 (10 or 30 mg/kg) every 3 days for 4 weeks. At 3 days after the last administration, mice were sacrificed. Tissues of livers were fixed with 4% paraformaldehyde, and liver sections were then stained with hematoxylin and eosin (A) or Azan (C). Hydroxyproline levels in the liver were assayed as described in Section 2 (C). Serum samples were used for measurement of ALT (B). (A and C) Data are representative of at least eight mice. (B) Data are means ± SEM ($n = 4$). *Significant difference vs. vehicle-treated group ($p < 0.05$).

failure (Fig. 3A). Histological analysis demonstrated that chronic exposure of SP70-induced denaturation of hepatocytes in a dose-dependent manner (Fig. 5A). Serum ALT levels were also elevated by SP70 administration (Vehicle, 14.3 KU; SP70, 24.8 and 42.1 KU at 10 and 30 mg/kg, respectively) (Fig. 5B). Liver fibrosis is a symptom of chronic liver injury, and thus, we investigated liver fibrosis. Collagen, which is accumulated in the fibrotic liver, was stained with Azan reagent, and blue-stained regions were observed in SP70-treated, but not vehicle-treated, liver sections (Fig. 5C). Elevated hydroxyproline content parallels the extent of fibrosis, and we investigated the hydroxyproline contents in the SP70-treated mouse liver. Injection of SP70 significantly elevated hepatic hydroxyproline contents 1.6- and 3.5-fold over control values, at 10 mg/kg and 30 mg/kg, respectively (Fig. 5D). These data indicate that chronic administration of SP70 causes liver fibrosis, even at doses that are non-toxic in a single injection.

4. Discussion

In the present study, we evaluated the acute toxicity of silica particles with a diameter of 70, 300 or 1000 nm, and we found that 70-nm silica particles injure the liver, but not the spleen, lung or kidney. Moreover, chronic administration of 70-nm silica particles caused liver fibrosis, even at doses that were non-toxic in a single injection.

Surface area is a critical factor for toxicity of nano-size particles in the liver. The numbers of particles of SP70, 300 and 1000 are 2.8×10^{12}, 3.5×10^{10} and 9.5×10^{8} particles/mg, respectively. The surface area of SP300 at 100 mg/kg, at which SP300 was not toxic, is similar to that of SP70 at 30 mg/kg, at which SP70 was toxic. Difference in the surface area may not affect the different toxicities in the liver between SP70 and 300.

Please cite this article in press as: H. Nishimori et al., Silica nanoparticles as hepatotoxicants, Eur. J. Pharm. Biopharm. (2009), doi:10.1016/j.ejpb.2009.02.005

There are highly specialized endothelial cells, LSECs, in the liver, and these separate sinusoidal blood from hepatocytes. Passage of particles through LSECs is the first step for translocation from the bloodstream to hepatocytes. LSECs have fenestrations with a diameter of 100 nm, and the liver injury seen with 70-nm silica particles may be due to the particle size. We investigated the role of LSECs in the particle-induced liver injury using CPA, a disruptor of LSECs [13–15]. Unexpectedly, the disruption of LSEC did not cause SP300- and SP1000-induced liver injury. These results were consistent with the previous report that disruption of LSECs by CPA did not affect the hepatocyte transduction of a lentivirus vector with a diameter of 120–200 nm larger than the fenestrations of LSECs [13]. In contrast, SP70-induced liver injury was dramatically suppressed by disruption of LSECs, and pores in the LSEC may be responsible for the hepatic toxicity of SP70. Spaces, called the space of Disse, exist between LSEC and hepatocytes [23]. Particles entering into these spaces can avoid efflux into the blood flow in the sinusoids of the liver, resulting that this may enhance interaction between the particles and hepatocytes. Thus, the Disse spaces between LSECs and hepatocytes may be responsible for the liver injury caused by SP70.

Resident macrophages in the liver, Kupffer cells play a pivotal role in defense against foreign particles by eliminating such particles via phagocytosis [17]. $GdCl_3$ has been widely used to block phagocytosis by Kupffer cells and to deplete Kupffer cells [12,13,20,21]. Inactivation of Kupffer cells had no effect on SP300 and SP1000 treatment, whereas pre-treatment with $GdCl_3$ led to increased liver injury by SP70. There is no evidence that $GdCl_3$ exerts any direct toxic effects on hepatocytes, LSECs, or on other cells in the liver [24]. Thus, the elevation of SP70 toxicity may be caused by the depletion of Kupffer cells. Depletion of Kupffer cells enhanced the transgene activity of adenovirus vectors with a similar size with SP70 in the liver [22]. Therefore, inhibition of phagocytosis of Kupffer cells may enhance the interaction between SP70 and hepatocytes by increase in SP70 moving into the Disse spaces. Inhalation of silica particles causes lung injury [25], and alveolar macrophages function as a defense against inhaled agents, including viruses and environmental particles, via phagocytosis [26]. Macrophage receptor with collagenous structure (MARCO), CD204 and CD36 are reported to be the receptors for inert particles [26–30]. Uptake of silica particles through MARCO or CD204 induces cytotoxicity in alveolar macrophages, leading to lung fibrosis [30,31]. Alveolar macrophages from BALB/c do not express MARCO and CD204, and silica particles are taken up through CD36 [30]. Thus, uptake of SP70 by Kupffer cells through CD36 might not trigger liver injury. In this study, we found that chronic administration of SP70 caused liver fibrosis, even at 10 mg/kg body weight, at which level acute liver injury was not observed after a single injection. Nano-size particles-induced continuous inflammation in the liver will cause liver fibrosis leading to hepatic cancer.

Further evaluation of relationship between toxicity and variety of sizes, shapes, and chemical modification on the surface of particles is needed, and the future studies based on these data will provide very useful information on future development of drug delivery system using nano-size materials.

Acknowledgements

The authors thank all members of our laboratory for their useful comments and discussion. This study was supported by a grant from the Ministry of Health, Labor, and Welfare of Japan.

References

[1] R.F. Service, U.S. nanotechnology. Health and safety research slated for sizable gains, Science 315 (2007) 926.
[2] A. Nel, T. Xia, L. Madler, N. Li, Toxic potential of materials at the nanolevel, Science 311 (2006) 622–627.
[3] G. Oberdorster, E. Oberdorster, J. Oberdorster, Nanotoxicology: an emerging discipline evolving from studies of ultrafine particles, Environ. Health Perspect. 113 (2005) 823–839.
[4] J.S. Kim, T.J. Yoon, K.N. Yu, B.G. Kim, S.J. Park, H.W. Kim, K.H. Lee, S.B. Park, J.K. Lee, M.H. Cho, Toxicity and tissue distribution of magnetic nanoparticles in mice, Toxicol. Sci. 89 (2006) 338–347.
[5] S. Takenaka, E. Karg, C. Roth, H. Schulz, A. Ziesenis, U. Heinzmann, P. Schramel, J. Heyder, Pulmonary and systemic distribution of inhaled ultrafine silver particles in rats, Environ. Health Perspect. 109 (Suppl. 4) (2001) 547–551.
[6] A. Nemmar, P.H. Hoet, B. Vanquickenborne, D. Dinsdale, M. Thomeer, M.F. Hoylaerts, H. Vanbilloen, L. Mortelmans, B. Nemery, Passage of inhaled particles into the blood circulation in humans, Circulation 105 (2002) 411–414.
[7] A. Nemmar, H. Vanbilloen, M.F. Hoylaerts, P.H. Hoet, A. Verbruggen, B. Nemery, Passage of intratracheally instilled ultrafine particles from the lung into the systemic circulation in hamster, Am. J. Respir. Crit. Care Med. 164 (2001) 1665–1668.
[8] M. Vallet-Regi, F. Balas, D. Arcos, Mesoporous materials for drug delivery, Angew. Chem. Int. Ed. Engl. 46 (2007) 7548–7558.
[9] S.D. Caruthers, S.A. Wickline, G.M. Lanza, Nanotechnological applications in medicine, Curr. Opin. Biotechnol. 18 (2007) 26–30.
[10] Z. Medarova, W. Pham, C. Farrar, V. Petkova, A. Moore, In vivo imaging of siRNA delivery and silencing in tumors, Nat. Med. 13 (2007) 372–377.
[11] M. Bottini, F. D'Annibale, A. Magrini, F. Cerignoli, Y. Arimura, M.I. Dawson, E. Bergamaschi, N. Rosato, A. Bergamaschi, T. Mustelin, Quantum dot-doped silica nanoparticles as probes for targeting of T-lymphocytes, Int. J. Nanomed. 2 (2007) 227–233.
[12] M.J. Hardonk, F.W. Dijkhuis, C.E. Hulstaert, J. Koudstaal, Heterogeneity of rat liver and spleen macrophages in gadolinium chloride-induced elimination and repopulation, J. Leukoc. Biol. 52 (1992) 296–302.
[13] N.P. van Til, D.M. Markusic, R. van der Rijt, C. Kunne, J.K. Hiralall, H. Vreeling, W.M. Frederiks, R.P. Oude-Elferink, J. Seppen, Kupffer cells and not liver sinusoidal endothelial cells prevent lentiviral transduction of hepatocytes, Mol. Ther. 11 (2005) 26–34.
[14] L.D. DeLeve, Cellular target of cyclophosphamide toxicity in the murine liver: role of glutathione and site of metabolic activation, Hepatology 24 (1996) 830–837.
[15] H. Malhi, P. Annamaneni, S. Slehria, B. Joseph, K.K. Bhargava, C.J. Palestro, P.M. Novikoff, S. Gupta, Cyclophosphamide disrupts hepatic sinusoidal endothelium and improves transplanted cell engraftment in rat liver, Hepatology 36 (2002) 112–121.
[16] K.I. Kivirikko, O. Laitinen, D.J. Prockop, Modifications of a specific assay for hydroxyproline in urine, Anal. Biochem. 19 (1967) 249–255.
[17] K. Decker, Biologically active products of stimulated liver macrophages (Kupffer cells), Eur. J. Biochem. 192 (1990) 245–261.
[18] K.T. Brunner, D. Hurez, C.R. Mc, B. Benacerraf, Blood clearance of P32-labeled vesicular stomatitis and Newcastle disease viruses by the reticuloendothelial system in mice, J. Immunol. 85 (1960) 99–105.
[19] L. Zhang, P.J. Dailey, A. Gettie, J. Blanchard, D.D. Ho, The liver is a major organ for clearing simian immunodeficiency virus in rhesus monkeys, J. Virol. 76 (2002) 5271–5273.
[20] R. Alemany, K. Suzuki, D.T. Curiel, Blood clearance rates of adenovirus type 5 in mice, J. Gen. Virol. 81 (2000) 2605–2609.
[21] A. Lieber, C.Y. He, L. Meuse, D. Schowalter, I. Kirillova, B. Winther, M.A. Kay, The role of Kupffer cell activation and viral gene expression in early liver toxicity after infusion of recombinant adenovirus vectors, J. Virol. 71 (1997) 8798–8807.
[22] G. Schiedner, S. Hertel, M. Johnston, V. Dries, N. van Rooijen, S. Kochanek, Selective depletion or blockade of Kupffer cells leads to enhanced and prolonged hepatic transgene expression using high-capacity adenoviral vectors, Mol. Ther. 7 (2003) 35–43.
[23] E. Wisse, R.B. De Zanger, K. Charels, P. Van Der Smissen, R.S. McCuskey, The liver sieve: considerations concerning the structure and function of endothelial fenestrae, the sinusoidal wall and the space of Disse, Hepatology 5 (1985) 683–692.
[24] R.M. Rai, S.Q. Yang, C. McClain, C.L. Karp, A.S. Klein, A.M. Diehl, Kupffer cell depletion by gadolinium chloride enhances liver regeneration after partial hepatectomy in rats, Am. J. Physiol. 270 (1996) G909–918.
[25] G.S. Cooper, F.W. Miller, D.R. Germolec, Occupational exposures and autoimmune diseases, Int. Immunopharmacol. 2 (2002) 303–313.
[26] M. Arredouani, Z. Yang, Y. Ning, G. Qin, R. Soininen, K. Tryggvason, L. Kobzik, The scavenger receptor MARCO is required for lung defense against pneumococcal pneumonia and inhaled particles, J. Exp. Med. 200 (2004) 267–272.
[27] L. Kobzik, Lung macrophage uptake of unopsonized environmental particulates. Role of scavenger-type receptors, J. Immunol. 155 (1995) 367–376.
[28] M.S. Arredouani, A. Palecanda, H. Koziel, Y.C. Huang, A. Imrich, T.H. Sulahian, Y.Y. Ning, Z. Yang, T. Pikkarainen, M. Sankala, S.O. Vargas, M. Takeya, K. Tryggvason, L. Kobzik, MARCO is the major binding receptor for unopsonized particles and bacteria on human alveolar macrophages, J. Immunol. 175 (2005) 6058–6064.
[29] A. Palecanda, J. Paulauskis, E. Al-Mutairi, A. Imrich, G. Qin, H. Suzuki, T. Kodama, K. Tryggvason, H. Koziel, L. Kobzik, Role of the scavenger receptor MARCO in alveolar macrophage binding of unopsonized environmental particles, J. Exp. Med. 189 (1999) 1497–1506.
[30] R.F. Hamilton Jr., S.A. Thakur, J.K. Mayfair, A. Holian, MARCO mediates silica uptake and toxicity in alveolar macrophages from C57BL/6 mice, J. Biol. Chem. 281 (2006) 34218–34226.
[31] R.F. Hamilton Jr., S.A. Thakur, A. Holian, Silica binding and toxicity in alveolarmacrophages, Free Radic. Biol. Med. 44 (2008) 1246–1258.

Please cite this article in press as: H. Nishimori et al., Silica nanoparticles as hepatotoxicants, Eur. J. Pharm. Biopharm. (2009), doi:10.1016/j.ejpb.2009.02.005

European Journal of Pharmaceutics and Biopharmaceutics xxx (2009) xxx–xxx

Contents lists available at ScienceDirect

European Journal of Pharmaceutics and Biopharmaceutics

journal homepage: www.elsevier.com/locate/ejpb

Note

Histological analysis of 70-nm silica particles-induced chronic toxicity in mice

Hikaru Nishimori [a], Masuo Kondoh [a,*], Katsuhiro Isoda [a], Shin-ichi Tsunoda [b,c], Yasuo Tsutsumi [b,c,d], Kiyohito Yagi [a]

[a] Laboratory of Bio-Functional Molecular Chemistry, Graduate School of Pharmaceutical Sciences, Osaka University, Osaka, Japan
[b] Laboratory of Pharmaceutical Proteomics, National Institute of Biomedical Innovation, Osaka, Japan
[c] The Center for Advanced Medicinal Engineering and Informatics, Osaka University, Osaka, Japan
[d] Laboratory of Toxicology, Graduate School of Pharmaceutical Sciences, Osaka University, Osaka, Japan

ARTICLE INFO

Article history:
Received 10 February 2009
Accepted in revised form 24 March 2009
Available online xxxx

Keywords:
Nanotoxicology
Silica particle
Histological analysis
Liver
Spleen

ABSTRACT

Nano-sized silica is a promising material for disease diagnosis, cosmetics and drugs. For the successful application of nano-sized material in bioscience, evaluation of nano-sized material toxicity is important. We previously found that nano-sized silica particles with a diameter of 70 nm showed acute liver failure in mice. Here, we performed histological analysis of major organs such as the liver, spleen, lung, kidney, brain and heart in mice, chronically injected with 70-nm silica particles for 4 weeks. Histological analysis revealed hepatic microgranulation and splenic megakaryocyte accumulation in these 70-nm silica particles treated mice, while the kidney, lung, brain and heart remained unaffected. Thus, liver and spleen appear to be the major target organs for toxicity by the chronic administration of the 70-nm silica particles.

1. Introduction

Recent progress in nanotechnology, the act of reducing size from the microscale to the nanoscale, has provided us with dramatic changes in industrial manufacturing and medicine. It also offers many benefits to revolutionize biotechnology, such as synthesis of new drugs with targeted delivery and regenerative medicine [1]. Reducing particle size increases surface area and makes modification of unique physicochemical properties, such as high conductivity, strength, durability, and chemical reactivity possible [2]. Thus, the nanotechnology has led to novel materials and innovations in the industry, bioscience and medicine.

Nanomaterials are already being used in bioscience and medicine, such as electronics, sunscreens, cosmetics and medicine for the purposes of diagnosis, imaging and drug delivery. For example, nano-sized silica particles are intended for the systemic and local delivery of drugs [3]. However, the toxicity of the manufactured nano-sized particles has not been fully evaluated.

We previously found that nano-sized particles with a diameter of 70 nm caused acute liver failure, while micro-sized particles with a diameter of 300 or 1000 nm did not [4]. In this study, we performed histological analysis of chronic toxicity induced by intravenous administration of 70-nm silica particles (SP70) for 4 weeks into the major organs, such as liver, lung, spleen, kidney, brain and heart of mice.

2. Materials and methods

2.1. Materials

Nano-sized silica particles with a diameter of 70 nm were obtained from Micromod Partikeltechnologie GmnH (Rostock, Germany). The surface was not modified. The mean diameters of these particles analyzed by Zetasizer (Sysmex Co., Kobe, Japan) were determined to be 55.7 nm. The particles were spherical and nonporous, and were stored at 25 mg/ml in aqueous suspension. The suspensions were thoroughly dispersed with sonication before use and diluted in water. The dispersion of the particles was confirmed by electron microscopy (data not shown). Reagents used were of research grade.

2.2. Animals

The 8-week-old BLAB/c male mice were purchased from Shimizu Laboratory Supplies Co., Ltd. (Kyoto, Japan), and housed in an environmentally controlled room at 23 ± 1.5 °C with a 12-h light/dark cycle. Mice had access to water and chow (Type MF, Oriental Yeast, Tokyo, Japan) *ad libitum*. Mice were intravenously

Abbreviations: SP70, 70-nm silica particles; HE, hematoxylin–eosin; ALT, alanine aminotransferase; HYP, hydroxyproline.

* Corresponding author. Laboratory of Bio-Functional Molecular Chemistry, Graduate School of Pharmaceutical Sciences, Osaka University, Suita, Osaka 565-0871, Japan. Tel.: +81 6 6879 8196; fax: +81 6 6879 8199.
E-mail address: masuo@phs.osaka-u.ac.jp (M. Kondoh).

0939-6411/$ - see front matter © 2009 Elsevier B.V. All rights reserved.
doi:10.1016/j.ejpb.2009.03.007

injected with vehicle or the particles twice a week for 4 weeks. On day 3 after the last injection, the mice were sacrificed, and the serum and organs were recovered. The experimental protocols conformed to the ethical guidelines of the Graduate School of Pharmaceutical Sciences, Osaka University.

2.3. Histological analysis

The liver, spleen, lung, kidney, brain and heart were removed and fixed with 4% paraformaldehyde. After sectioning, thin sections of tissues were stained with hematoxylin and eosin for histological observation.

2.4. Biochemical analysis

Serum alanine aminotransferase (ALT) was measured using a commercially available kit according to the manufacturer's protocol (Wako Pure Chemical, Osaka, Japan).

2.5. Hydroxyproline (HYP) assay

Hepatic HYP content was measured by Kivirikko's method with some modification [5]. Briefly, liver tissue was hydrolyzed in 6 M HCl at 110 °C for 24 h. The resultant supernatant was neutralized with 8 N KOH, and then 2 g of KCl and 1 ml of 0.5 M borate buffer were added, followed by a 15-min incubation at room temperature and further incubation for 15 min at 0 °C. Chloramines-T solution was then prepared and added. After additional incubation for 1 h at 0 °C, 2 ml of 3.6 M sodium thiosulfate was added, followed by incubation at 120 °C for 30 min. Next, 3 ml of toluene was added with incubation for a further 20 min at room temperature. After centrifugation, 2 ml of the resultant supernatant was added to Ehrlich's reagent, followed by incubation for 30 min at room temperature. Subsequently, absorbance was measured at 560 nm.

2.6. Statistical analysis

Statistical analysis was performed by Student's *t*-test. The level of significance was set at $p < 0.05$.

3. Results and discussion

We previously found that intravenous administration of SP70 induced liver injury through a single administration [4]. To investigate the chronic toxicity of SP70, 10 or 30 mg/kg of SP70 was intravenously injected into mice twice a week for 4 weeks at which point the livers were not injured or injured by the single injection, respectively [4]. During chronic administration, no significant differences were observed in the body weight between the vehicle and the SP70-treated group (Fig. 1) and no abnormal behaviors were detected (data not shown). Therefore, SP70 treatment did not show apparent toxicity in mice at the low dose.

Next, we performed histological analysis of tissues that are enriched with reticuloendothelial system (RES) such as the liver, spleen, and lungs and non-RES organs such as the heart, kidney and brain. As shown in Fig. 2A and B, treatment with SP70 induces hepatic microgranulation and increases splenic megakaryocyte accumulation. In contrast, the remaining RES organ, the lung, and all the non-RES organs did not show tissue injury with SP70 treatment (Fig. 2B–F). Thus, we examined a serum biochemical marker of liver injury, ALT, to confirm liver injury. SP70 treatment significantly elevated serum ALT levels (Fig. 3A), but a renal injury marker, blood urea nitrogen, was not elevated by these treatments

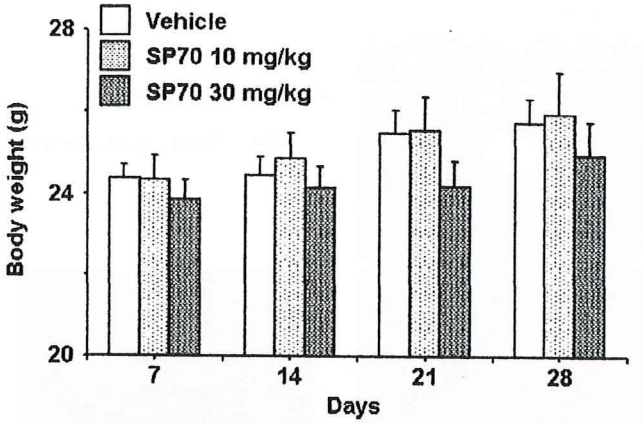

Fig. 1. Body weight changes in mice treated with SP70 for 4 weeks. Mice were intravenously administered SP70 at 0, 10 or 30 mg/kg twice a week for 4 weeks. The body weights of the treated mice were monitored on days 7, 14, 21 and 28. Each point represents mean ± SEM ($n = 5–7$).

(data not shown). Chronic hepatic injury causes liver fibrosis, finally leading to hepatic carcinoma. The chronic treatment with SP70 also elevated a marker of fibrosis, HYP, in the liver (Fig. 3B). Taken together, chronic SP70 treatment appears to injure the liver and spleen.

As innovative materials cover wide fields from industry to life science, nanomaterials have potential to improve the quality and performance of many consumer products as well as medical therapies. Thus, it is very critical in the field of nanotechnology to also assess the risk of nano-sized materials. As the use of nano-sized silica particles in cosmetics and the application in pharmaceutical research, e.g., drug delivery and molecular imaging [3,6] are increasing, we evaluated the toxicity of nano-sized silica particles. We have already found that SP70 causes acute liver injury in mice [4]. In the present study, we evaluate the influence of chronic administration of SP70 for 4 weeks on major organs by histological analysis. As the nano-sized particles are taken into RES organs such as the liver, lung and spleen, we expected that all the RES organs would be injured by chronic SP70 exposure. However, histological abnormalities in the lung were not observed. Kim et al. found that 50-nm silica particles were distributed into all the RES organs, but the amount of the distributed particles into the lung was smaller than that into the liver and spleen [7]. Therefore, the lack of histological abnormalities in the lung may be due to a lower distribution of SP70.

The underlying mechanism for histological injury in the liver and spleen remains to be elucidated. We previously found that the serum levels of inflammatory cytokines (interleukin-6 and tumor necrosis factor-α) were elevated by SP70 [4]. Uptake of SP70 by macrophages in the liver and spleen may cause the release of the cytokines from the macrophage, leading to histological abnormalities. Macrophage receptor with collagenous structure (MARCO), CD204 and CD36 are all macrophage silica particle receptors [8–10]. CD36 is expressed in macrophages of BALB/c mice [10].

In the present study, there is no observation of histological injury in lung, kidney, brain and heart. Regulation of liver and spleen injuries may be critical for the safe application of these nano-sized silica particles. Future analysis is necessary to determine tissue distribution of SP70. Extensive studies are also required to provide the basis for a new class of nanomaterials for drugs, proteins, and gene delivery applications. We are developing materials and methods to control the bio-distribution of these nano-sized silica particles.

Please cite this article in press as: H. Nishimori et al., Histological analysis of 70-nm silica particles-induced chronic toxicity in mice, Eur. J. Pharm. Biopharm. (2009), doi:10.1016/j.ejpb.2009.03.007